

Sodium metasomatism along the Melones Fault Zone, Sierra Nevada Foothills, California, USA

GEORGE V. ALBINO*

Corona Gold Inc., 1375 Greg Street, Suite 105, Sparks, NV, 89431, USA

Abstract

Albite, locally aegirine- and riebeckite-bearing, formed as a result of sodium metasomatism of felsic dykes and argillites along the Melones Fault Zone near Jamestown, California. Pyrite, magnetite, hematite and titanite are common in small amounts in altered dykes. The dykes were originally plagioclase–hornblende porphyritic, and had major and trace element abundances typical of calc-alkaline rocks, whereas they now have Na₂O contents as high as 11.40%. Associated fracture-filling veins are dominated by albite, but locally include aegirine, analcime, paragonite, calcite and sodic scapolite. Quartz is present in most albitic rocks, but is absent in riebeckite- and aegirine-bearing samples. Albitization predated CO₂ metasomatism and formation of sericite-pyrite assemblages that are typical of gold deposits of the Mother Lode Belt.

Alkaline fluids responsible for Na-metasomatism had elevated Na⁺/K⁺ and Na⁺/H⁺, relatively high f_{O_2} , and low $a_{H_4SiO_4}$. The presence of titanite indicates fluid X_{CO_2} was low, in contrast to fluids that formed later carbonate-bearing assemblages. Sodic scapolite suggests that, at least locally, the fluids attained very high salinities.

Mass balance calculations indicate that alteration involved addition of large amounts of sodium, and the removal of SiO₂ and K₂O. Textural preservation, combined with volume factors calculated from specific gravity and whole rock analytical data, indicate that Na-metasomatism was essentially isovolumetric.

Sodium-rich zones along the Melones Fault Zone are closely associated with fault-bounded bodies of ultramafic rock, typically altered to talc-carbonate or quartz-magnesite-Cr muscovite assemblages. Carbonatization and talc-forming reactions in the ultramafic rocks may lead to SiO₂-undersaturated fluids. Expansion of the muscovite stability field in terms of Na⁺/K⁺-Na⁺/H⁺, as a result of incorporation of Cr (up to 7.7% Cr₂O₃) in muscovite, would result in H⁺- and K⁺-depletion as the fluid interacts with ultramafic rocks. This could lead to fluids with elevated Na⁺/K⁺ and high pH, as documented in this occurrence.

KEYWORDS: sodium metasomatism, fault zone, Sierra Nevada, California.

Introduction

MAJOR fault zones are commonly the locus for large-scale fluid movement in the crust, resulting in mass transfer and associated formation of metasomatic mineral assemblages. Mesothermal gold-quartz veins along major faults (e.g. Colvine, 1989; Card *et al.*,

1989; Groves *et al.*, 1989) are typically associated with extensive zones of CO₂ and locally alkali metasomatism, which result in formation of white mica and calcite-, ankerite-, or magnesite-bearing assemblages (Kerrich, 1983). Albitic zones are also common in these deposits (e.g. Coveney, 1981; Couture and Pilote, 1993; Kishida and Kerrich, 1987), and where paragenetic relationships can be determined, typically appear to have formed prior to sericitic assemblages (Albino, 1990; Kishida and Kerrich, 1987). In a few instances (e.g. Morasse *et*

* Present address: U.S. Geological Survey, P.O. Box 1488, Jeddah 21431, Saudi Arabia

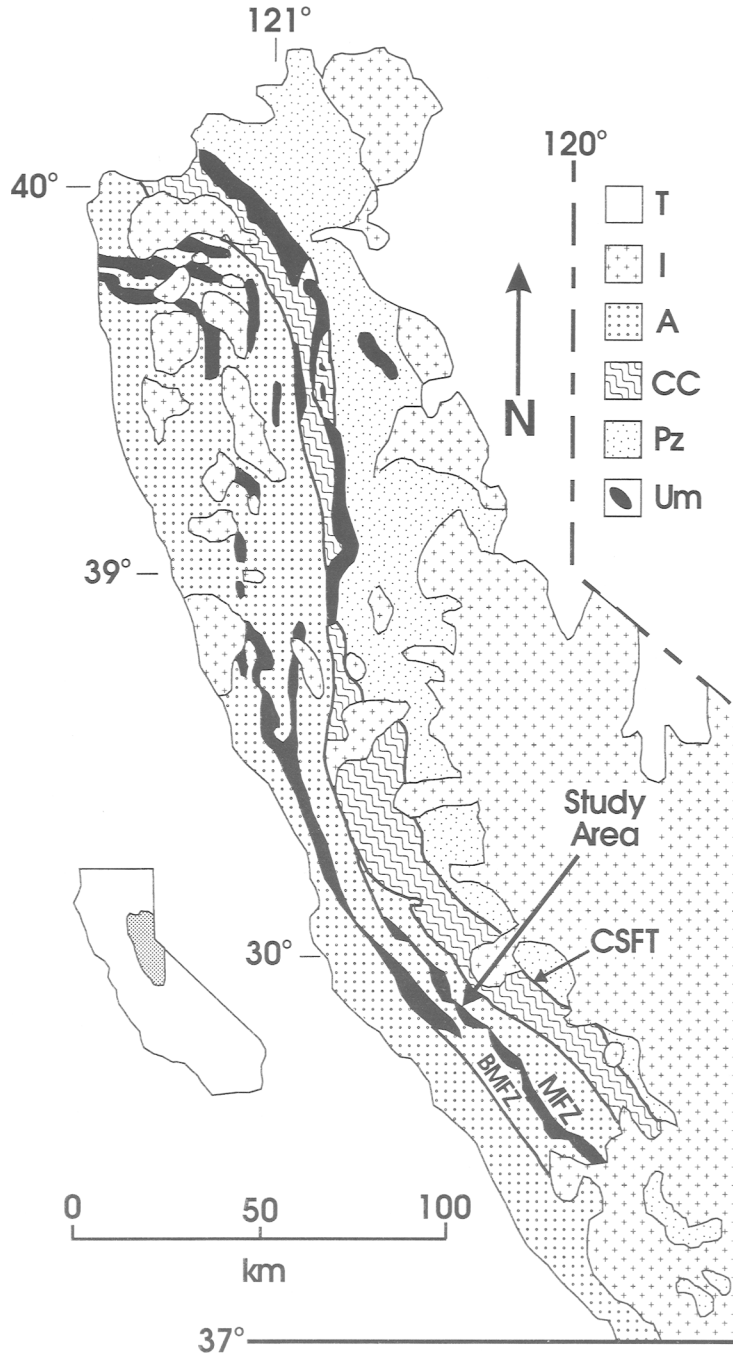


FIG. 1. Generalized geological map of the western Sierra Nevada (after Albino, 1993) showing broad-scale division of pre-Cretaceous rocks into eastern Paleozoic belt (Pz), central belt of Calaveras Complex (CC) separated by Calaveras-Shoo Fly thrust (CSFT), and western Triassic to Jurassic arc (A). Ultramafic rocks (Um) lie along major faults, including the Melones fault zone (MFZ) and Bear Mountain fault zone (BMFZ). Pre-Cretaceous rocks are intruded by Jurassic to Cretaceous plutons (I), and all units are overlain by Tertiary to Recent cover (T). Sodium-metasomatized zones are along the Melones fault zone at location shown.

al., 1988), including the one described below, Na-metasomatism has led to formation of assemblages including sodic amphiboles and/or pyroxenes, in addition to albite. These rare occurrences indicate that fluids of rather extreme composition were present at times in the hydrothermal systems. It is the purpose of this paper to present new information on the nature of sodic altered rocks along the Melones Fault Zone (Turner, 1896; Ransome, 1900; Knopf, 1929; Leonardos and Fyfe, 1967), and to suggest a mechanism to account for the origin of the metasomatic fluids. Note that the proposed mechanism is very similar to that proposed by Böhlke (1986, 1989), who studied albitic zones in the Alleghany gold district, approximately 200 km north of the study area.

Geological setting

The Na-metasomatized zones are present along the Melones Fault Zone (Fig. 1), a major structure in the western Sierra Nevada metamorphic belt (SNMB). The SNMB is composed of three main blocks (Albino, 1993, and references therein): (1) an eastern deformed belt consisting mainly of Lower Paleozoic metasedimentary rocks (Shoo Fly Complex) metamorphosed to upper greenschist facies; (2) a central belt made up of an oceanic assemblage (including ophiolite fragments) of Upper Paleozoic to Triassic age (Calaveras Complex); and (3) an arc assemblage of Late Triassic and Jurassic age consisting of basaltic andesite to rhyolite flows and tuffs, overlain by argillite and quartz-rich siltstone and wacke, all metamorphosed under sub-greenschist to lower greenschist conditions. These major subdivisions are separated by low-angle faults (Calaveras-Shoo Fly Thrust and the 'ancestral' Sonora Fault), which have largely been obscured by later high-angle faults. These high-angle faults belong to the Foothills fault system (Clark, 1960), and include the Sonora Fault and the Melones and Bear Mountain Fault Zones. The latter two structures divide the Triassic–Jurassic arc terrane into blocks of contrasting metamorphic grade and structural history. The Melones and Bear Mountain Fault Zones are marked along much of their lengths by fault-bounded slivers of serpentinized ultramafic rocks, and phyllonite derived from metasedimentary and meta-volcanic rocks of the Calaveras Complex. In places, particularly in the southern portion of the SNMB, the faults host narrow dykes, which appear to post-date most deformation along the faults, but are sheared or folded locally. The dykes range in composition from pyroxenitic to granodiorite, with medium-grained equigranular to plagioclase-hornblende porphyritic diorite(?) most abundant. The absolute ages of the dykes are unknown, but the compositional range, and

timing relative to deformation suggest that the dykes may be related to the Guadeloupe pluton, emplaced at approximately 150 Ma (Saleeby *et al.*, 1989).

Sodium-metasomatized zones

Strongly Na-metasomatized zones are present in intermediate dykes and phyllonite of the Calaveras Complex along the Melones Fault Zone near Jamestown (Lamarre, 1977), and in the area of the former town of Moccasin, now covered by the New Melones Reservoir (Leonardos and Fyfe, 1967; Knopf, 1929). At Jamestown the Na-rich zones (Fig. 2) are developed mainly in phyllonite derived from the argillite of the Calaveras Complex, in close association with large fault blocks of ultramafic rocks, altered mainly to talc–dolomite or magnesite–quartz. The Na-rich rocks consist of finely banded albite–pyrite–titanite or rutile \pm quartz \pm chlorite rock, which closely preserves textures of the precursor metasedimentary rocks (Fig. 3). These rocks contain up to 9.4% Na₂O, in contrast to the approximately 2–4% typical of unaltered argillite of the region. The reverse is true for K, which is much less abundant in albitized rock than in unaltered argillite. Pyrite is one of the main constituents of the albitized argillite, making up as much as 10% of the rock. The greater abundance of Fe in albitized, as compared with fresh argillite, suggests that it, too, along with S, was added during alteration.

At Moccasin the altered rocks include intermediate dykes, and metasedimentary rocks of the Calaveras Complex. As at Jamestown, the Na-rich zones are along the margin of altered ultramafic bodies (Fig. 4). Three main assemblages are noted in the altered dykes: (1) albite (quartz–pyrite–chlorite); (2) albite–riebeckite (–aegirine), and (3) albite–aegirine \pm hematite or magnetite (Fig. 5). Quartz and pyrite are absent in Na-pyroxene and amphibole-bearing rocks. Discontinuous exposure in the area prevents delineation of zoning patterns, but the occurrence of the assemblages becomes increasingly restricted in the order albite (–quartz–chlorite–pyrite) \rightarrow albite–riebeckite \rightarrow albite–aegirine (\pm iron oxide). Fracture-filling veins (Fig. 5D) within the dykes, and in adjacent gabbro outcrops contain the assemblages albite–chlorite, albite–aegirine, and albite–analcime–paragonite–marialitic scapolite.

Albite makes up the bulk of most of the altered rocks, occurring as pseudomorphs of plagioclase phenocrysts, and as xenomorphic grains forming a fine-grained granular groundmass. It is very abundant as a fracture-filling phase in Na-altered rocks, and in adjacent gabbro or little-altered dykes. It occurs as monominerallic veins (commonly with tabular, 'cleavelandite'-like morphology) or in combination with carbonate minerals or aegirine. Sericite altera-

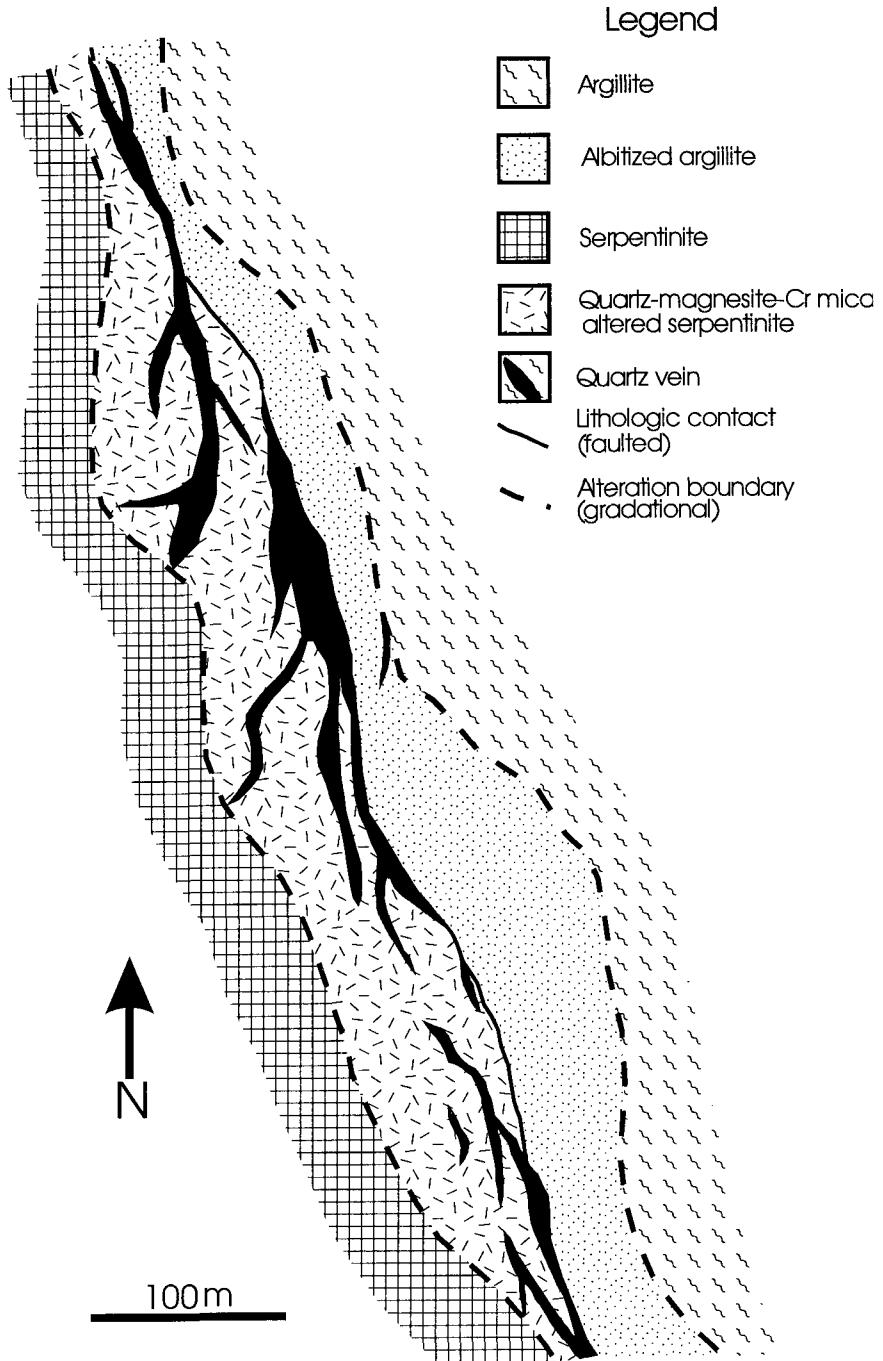


FIG. 2. Geologic sketch map of part of Jamestown area (modified from Lamarre, 1977), showing location of albitized argillite and quartz-magnesite-Cr mica altered ultramafic rocks of Calaveras Complex, adjacent to faulted argillite-serpentinite contact. Major quartz veins, which post-date most alteration, are localized along this contact and in altered ultramafic rocks.

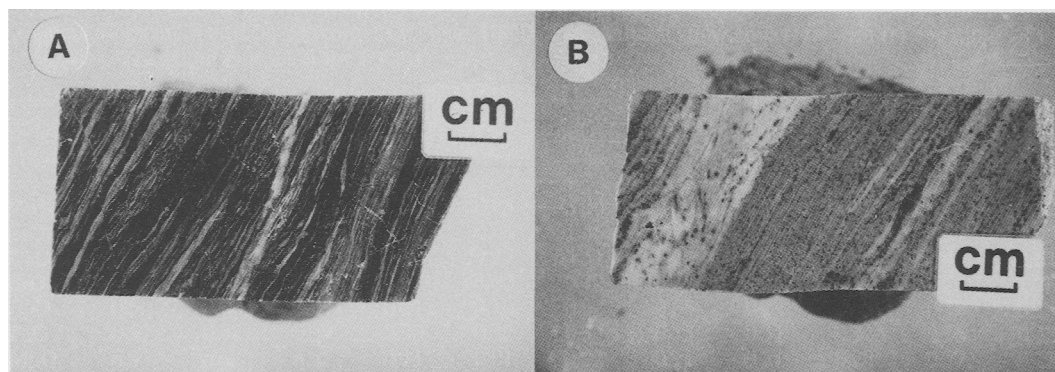


FIG. 3. (A) – Typical unaltered, carbonaceous phyllite (argillite), Jamestown area; (B) – Intensely albitized argillite near contact with ultramafic rocks, Jamestown area. Dark specks are hydrothermal pyrite.

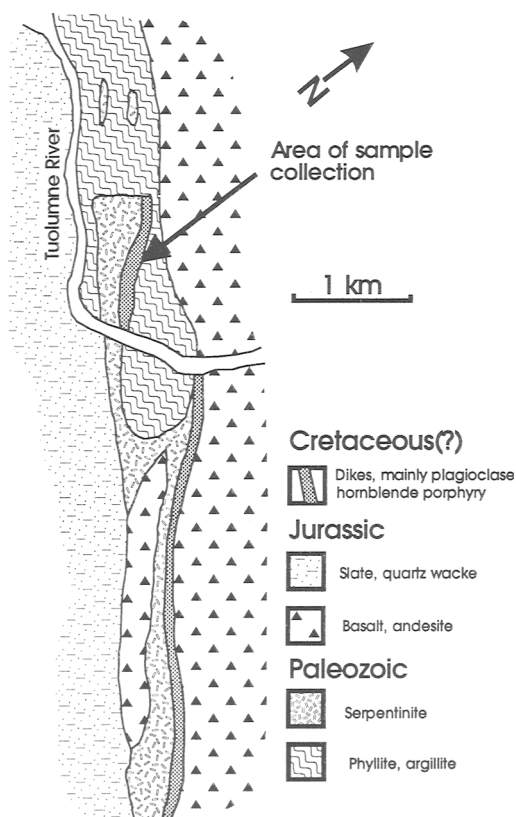


FIG. 4. Geologic sketch map of Moccasin area showing dyke along the faulted contact between serpentinite and Jurassic(?) mafic volcanic and lesser metasedimentary rocks. Location of the samples studied, indicated by arrow.

tion, locally with associated calcite or dolomite, is commonly superimposed on early albite.

Riebeckite occurs most commonly as irregular bundles of elongate prisms, pseudomorphous after hornblende, and as fine needles in groundmass (Fig. 5). In altered phyllitic rocks it forms felted to nematoblastic aggregates, commonly preferentially replacing specific beds or lamellae.

Aegirine is present as pseudomorphs after hornblende, disseminated in the albitic groundmass, or as rims on earlier-formed magnetite (Fig. 5). It ranges in habit from stubby to highly elongate prismatic. It is fairly common as a fracture-filling mineral, occurring with albite.

Mineral chemistry

Analytical techniques. Compositions of sodic alteration minerals were determined by electron microprobe analysis at the University of Western Ontario. Two instruments were used, an MAC 400 microprobe equipped with automated spectrometers and Krisel controller, and a JEOL 8600 Superprobe. Quantitative results presented below are based on wavelength-dispersive analysis, using a variety of natural mineral standards. Operating conditions were 15 kV accelerating voltage, with a specimen current of approximately 10 nA. On the MAC instrument, counts were recorded for 30 s, or until 10,000 counts were recorded. For the analyses on the JEOL instrument, the counting time was 20 s, or until a standard deviation of 1% for count rates was achieved.

Energy-dispersive (semi-quantitative) techniques were used in determination of plagioclase and scapolite compositions. Plagioclase was uniformly observed to be pure albite, at the detection limit of

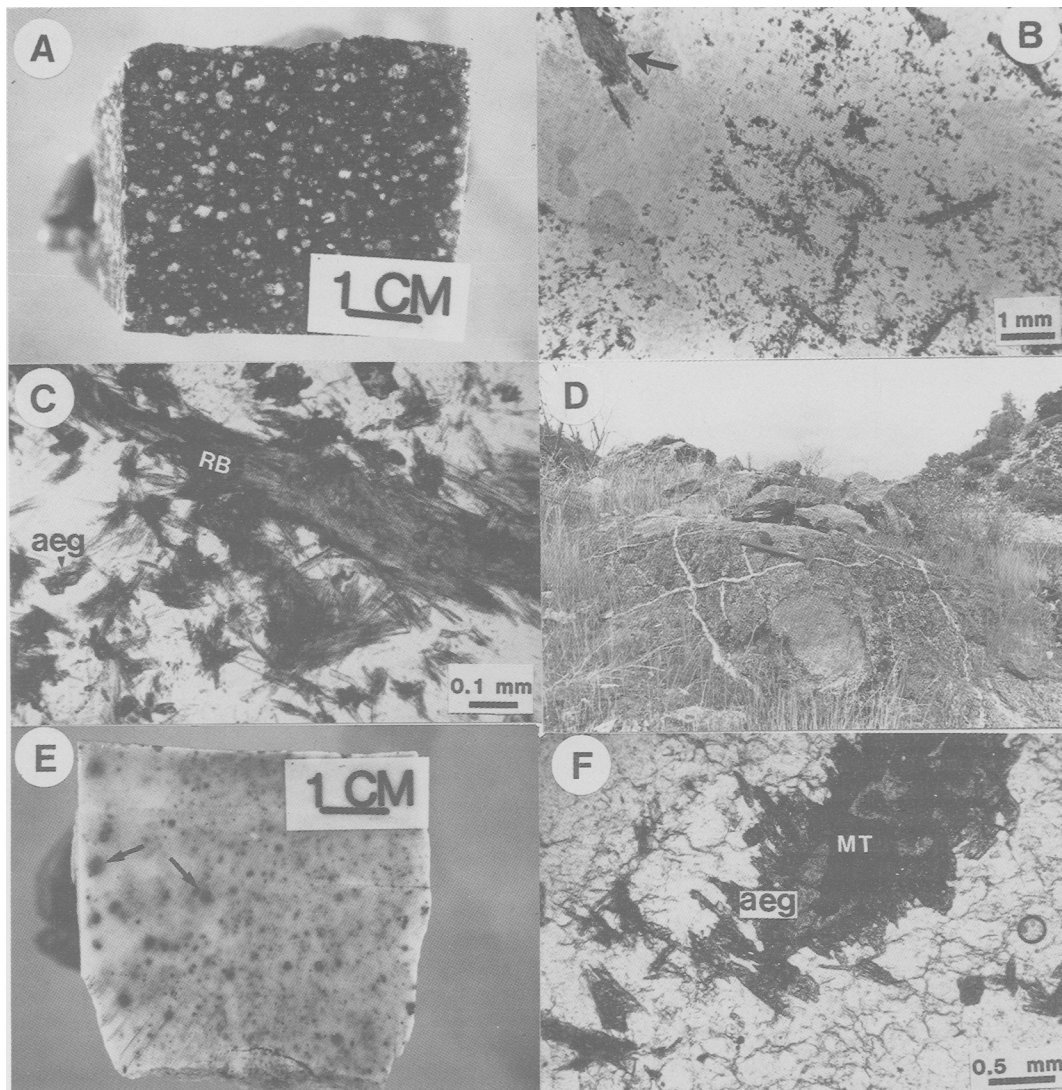


FIG. 5. Sodium-metasomatized rocks from Moccasin area. (A) plagioclase-hornblende porphyritic dyke with dark groundmass resulting from riebeckite alteration; (B) photomicrograph of sample in A, showing riebeckite as pseudomorphs after hornblende phenocrysts (arrow), with preservation of primary hornblende morphology; (C) detail of B, showing felted texture of secondary riebeckite (RB), and minor aegirine (aeg) in groundmass; (D) gabbro along Melones fault zone cut by albite±analcime veins. Altered dyke exposed upper right-hand corner of photograph; (E) albite-aegirine altered dyke. Black spots are magnetite rimmed by aegirine; (F) photomicrograph of sample in E showing aegirine prisms (aeg) as overgrowths on magnetite (MT).

EDS analysis (approximately 0.5%). Scapolite was apparently close to end-member marialite.

Amphiboles. Composition data for sodic amphiboles from one sample (5-10-2C) are presented in Table 1, and illustrated in Fig. 6. Two compositional groups are evident, one magnesio-riebeckite with $Fe^{3+}/(Fe^{3+}+Al^{vi})$ near 0.9 and variable

$Mg/(Mg+Fe^{2+})$, and the other crossite to eckermannite, with significantly lower $Fe^{3+}/(Fe^{3+}+Al^{vi})$ and $Mg/(Mg+Fe^{2+})$. The moderate to high values of $Fe^{3+}/(Fe^{3+}+Al^{vi})$ indicate that the alkali amphiboles are not indicative of formation under elevated pressure (Robinson *et al.*, 1982). The range in composition of the riebeckites is similar to those

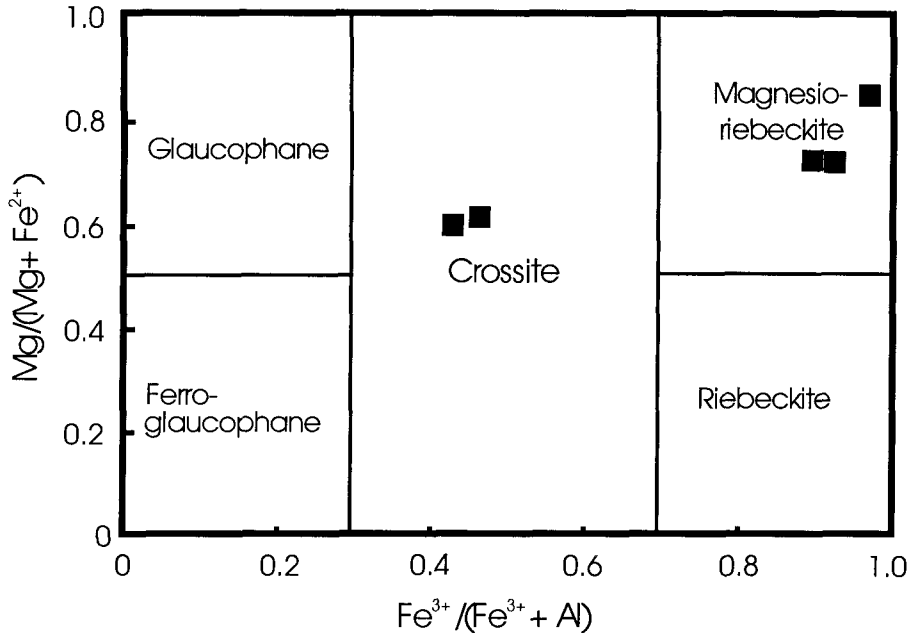


FIG. 6. Compositions of metasomatic amphibole in terms of $Mg/(Mg+Mn+Fe^{2+})$ vs $Fe^{3+}/(Fe^{3+}+Al^{vi})$ (after Leake, 1978). Note two distinct populations, falling in crossite and magnesio-riebeckite fields.

from the magnetite-hematite-bearing transitional blueschist-greenschist of the Shuksan suite, northern Washington state, in accordance with observations of magnetite and hematite in the altered dykes (Okay, 1980). The alkali amphiboles of the Na-metasomatized rocks contrast with primary igneous, and minor secondary amphiboles from unaltered dykes (Table 1), which are tschermakitic hornblende and actinolite, respectively.

Pyroxenes. Pyroxenes from three samples containing albite-aegirine and albite-riebeckite-aegirine assemblages were analysed (Table 2). There is considerable range in composition, from nearly end-member acmite (e.g. sample 5-10-6) and aegirine-augite with 0.7 to 0.8 mole fraction acmite. Pure acmite is found as a fracture-filling mineral, whereas aegirine-augite is typical of pyroxenes formed by alteration of pre-existing rocks. The aegirine-augites have low to moderate Al, between 0.03 and almost 0.5 atoms per formula unit (p.f.u.). Titanium ranges from <0.01 to 0.07 atoms p.f.u., and has a general negative correlation with the acmite component. Calculating compositions of the aegirine-augites in terms of conventional end-members is difficult, as Na is present in excess of $Al+Fe^{3+}$ in almost all analyses. In addition, the titanium contents of the aegirine-augites are very high (up to 2.65 wt.

% = 0.074 atoms p.f.u), and the substitutional mechanisms for Ti are uncertain, as there is insufficient Ca or Al to allow substitutions of the type proposed by Papike and White (1979). The excess Na, combined with a generally positive correlation between Ti and Mg, and a negative correlation between Ti and Si suggests that a coupled substitution involving Na, Mg and Ti, resulting in a hypothetical end-member of the form $(Na_2MgTi)-(TiSi_3)O_{12}$, may account for some compositional variation in the aegirine-augites.

Analcime and Na-Mica. Analcime, accompanied by a white mica, and locally NaCl-rich scapolite (identified optically and by qualitative energy-dispersive analysis) occur with albite as fracture-fillings in Na-metasomatized dykes and more commonly in adjacent gabbro (Fig. 5). The analcime is near end-member in composition, with minor substitution of K for Na (Table 3). Similarly, the white mica is virtually pure end-member paragonite (Table 3).

Geochemistry

The mineralogical changes described above were accompanied by major changes in bulk composition of the altered rocks (Tables 4 and 5). Unaltered dykes

TABLE 1. Compositions of primary and metasomatic amphibole in intermediate dykes near Moccasin, California

Sample Analysis	6-7-1 prim?	6-7-1 prim	6-7-1 sec	6-7-1 prim	6-7-1 prim	6-7-1 prim	5-10-2C rieb				
SiO ₂	45.16	45.64	54.95	46.96	46.73	56.05	55.40	55.26	56.42	56.45	56.88
TiO ₂	1.69	1.92	0.01	1.25	1.11	0.17	0.27	0.09	0.09	0.18	0.25
Al ₂ O ₃	11.58	10.81	0.71	10.48	10.51	0.91	2.70	1.03	0.75	1.26	4.57
Cr ₂ O ₃	0.14	0.20	0.11	0.06	0.17	0.05	0.09	0.05	0.04	0.07	0.11
FeO	8.89	8.94	13.75	10.24	10.99	13.77	15.72	18.44	20.57	19.35	17.36
MnO	0.05	0.10	0.60	0.16	0.07	0.09	0.01	0.09	0.04	0.02	0.00
MgO	16.84	16.44	14.72	15.63	15.77	16.47	10.65	12.88	11.52	12.27	10.56
CaO	11.31	11.59	12.59	11.45	11.72	2.39	4.28	0.89	0.72	0.58	1.64
Na ₂ O	2.34	2.21	0.18	1.75	2.38	6.95	8.49	7.43	7.84	8.89	7.69
K ₂ O	0.36	0.42	0.09	0.45	0.35	0.27	0.12	0.11	0.02	0.07	0.09
Total	98.36	98.27	97.71	98.43	99.80	97.12	97.73	96.27	98.01	99.14	99.15
atoms on the basis of 23 O											
Si	6.328	6.446	7.953	6.614	6.543	7.799	8.000	7.871	7.989	7.924	7.968
Ti	0.178	0.204	0.001	0.132	0.117	0.018	0.029	0.010	0.010	0.019	0.026
Al	1.913	1.800	0.121	1.740	1.735	0.149	0.460	0.173	0.125	0.209	0.755
Cr	0.016	0.022	0.013	0.007	0.019	0.006	0.010	0.006	0.004	0.008	0.012
Fe ³⁺	1.042	1.056	1.664	1.206	1.287	1.576	0.366	1.718	1.498	1.292	0.646
Fe ²⁺	0.006	0.012	0.074	0.019	0.008	0.026	1.532	0.478	0.938	0.980	1.388
Mn	3.517	3.460	3.175	3.281	3.291	0.011	0.001	0.011	0.005	0.002	0.000
Ca	1.698	1.754	1.952	1.728	1.758	3.415	2.292	2.734	2.431	2.567	2.205
Na	0.636	0.605	0.051	0.478	0.646	0.356	0.662	0.136	0.109	0.087	0.246
K	0.064	0.076	0.017	0.081	0.063	1.875	2.377	2.052	2.153	2.420	2.089
Fe ³⁺ /Fe ³⁺ +Al ^{VI}	-	-	-	-	-	0.048	0.044	0.020	0.004	0.013	0.016
Mg/Mg+Fe ²⁺	0.77	0.77	0.66	0.73	0.72	0.91	0.44	0.91	0.92	0.86	0.46

Notes

- prim = primary igneous, sec = secondary overgrowth, rieb = blue-grey alkali amphibole
- atomic proportions calculated on the basis of 13 cations, exclusive of Ca, Na, and K

TABLE 2. Compositions of Na-pyroxenes in altered intermediate dykes near Moccasin, California

Sample Analysis	5-10-2C 1	5-10-2C 2	5-10-2B 1	5-10-2B 2	5-10-2B 2	5-10-2B 2-rim	5-10-6 1	5-10-6 1	5-10-6 2							
SiO ₂	55.69	53.62	53.49	52.17	58.24	52.34	51.59	53.44	54.10	51.69	50.40	51.97	50.40	51.69	50.40	51.97
TiO ₂	0.33	2.30	1.41	1.87	1.84	2.65	2.39	2.62	1.60	0.05	0.06	1.83	0.06	0.05	0.06	1.83
Al ₂ O ₃	5.39	0.96	0.90	0.67	10.85	0.81	0.64	0.68	1.55	0.20	0.30	0.31	0.30	0.20	0.30	0.31
Cr ₂ O ₃	0.08	0.07	0.09	0.07	0.08	0.04	0.11	0.05	0.05	0.05	0.04	0.00	0.04	0.05	0.04	0.00
MnO	0.25	0.08	0.18	0.28	0.14	0.13	0.32	0.57	0.13	0.05	0.04	1.53	0.04	0.05	0.04	1.53
FeO	11.51	19.82	19.06	21.20	11.56	18.89	16.87	17.86	18.39	31.25	31.46	21.10	31.46	31.25	31.46	21.10
MgO	7.95	5.52	5.47	4.57	3.90	5.08	6.51	6.15	5.60	0.32	0.32	4.25	0.32	0.32	0.32	4.25
CaO	10.68	6.91	8.19	6.06	3.27	6.64	8.55	8.51	7.71	0.69	0.47	7.91	0.47	0.69	0.47	7.91
Na ₂ O	8.02	11.14	10.79	11.25	10.74	11.43	10.20	9.57	10.42	14.86	15.21	10.05	15.21	14.86	15.21	10.05
K ₂ O	0.04	0.04	0.03	0.02	0.07	0.04	0.03	0.02	0.02	0.04	0.04	0.03	0.02	0.04	0.04	0.03
Total	99.94	100.46	99.61	98.16	100.69	98.05	97.21	99.47	99.57	99.20	98.34	98.98	98.34	99.20	98.34	98.98
atoms on the basis of 6 O																
Si	2.006	1.942	1.952	1.941	2.071	1.936	1.924	1.970	1.977	1.910	1.872	1.943	1.872	1.910	1.872	1.943
Ti	0.009	0.063	0.039	0.052	0.049	0.074	0.067	0.073	0.044	0.001	0.002	0.051	0.002	0.001	0.002	0.051
Al	0.229	0.041	0.039	0.029	0.455	0.035	0.028	0.030	0.067	0.009	0.013	0.014	0.013	0.009	0.013	0.014
Cr	0.001	0.001	0.002	0.001	0.001	0.001	0.002	0.001	0.001	0.001	0.001	0.000	0.001	0.001	0.001	0.000
Mn	0.008	0.002	0.006	0.009	0.004	0.004	0.010	0.018	0.004	0.002	0.001	0.048	0.001	0.002	0.001	0.048
Fe ²⁺	0.347	0.600	0.582	0.660	0.344	0.584	0.526	0.551	0.562	0.966	0.977	0.660	0.977	0.966	0.977	0.660
Fe ³⁺	0.000	0.000	0.000	0.000	0.000	0.000	0.000	0.000	0.000	0.000	0.000	0.000	0.000	0.000	0.000	0.000
Mg	0.427	0.298	0.297	0.253	0.207	0.280	0.362	0.338	0.305	0.018	0.018	0.237	0.018	0.018	0.018	0.237
Ca	0.412	0.268	0.320	0.242	0.125	0.263	0.342	0.336	0.302	0.027	0.019	0.317	0.019	0.027	0.019	0.317
Na	0.560	0.782	0.763	0.812	0.741	0.820	0.738	0.684	0.738	1.065	1.095	0.729	1.095	1.065	1.095	0.729
K	0.002	0.002	0.001	0.001	0.003	0.002	0.001	0.001	0.001	0.002	0.002	0.001	0.001	0.002	0.002	0.001

Note - oxides in wt. %

TABLE 3. Composition of analcime and paragonite, sample 5-10-8B

Mineral	analcime	analcime	paragonite	paragonite
Na ₂ O	12.89	12.82	8.00	8.16
MgO	0.02	0.03	0.00	0.16
Al ₂ O ₃	21.39	24.06	38.00	38.34
SiO ₂	53.82	53.99	45.57	45.92
K ₂ O	0.69	1.07	0.08	0.06
CaO	0.01	0.00	0.57	1.38
TiO ₂	0.30	0.00	0.00	0.00
Cr ₂ O ₃	0.00	0.00	0.00	0.04
MnO	0.00	0.00	0.00	0.00
FeO	0.00	0.00	0.00	0.03
Total	89.12	91.97	92.22	94.09
atoms per formula unit				
Na	0.95	0.91	1.02	1.03
Al	0.96	1.04	2.96	2.94
Si	2.04	1.98	3.01	2.99
K	0.03	0.05	0.01	0.01
Ca	0.00	0.00	0.04	0.10

– oxides in wt. %

– number of atoms calculated on the basis of 6 O (analcime) and 11 O (paragonite)

have Na₂O between 5.0 and 6.7 wt. %, in contrast to as much as 11.4 wt. % in aegirine-riebeckite-bearing samples (Table 4). This change is accompanied by decreases in K₂O and SiO₂ to <0.2 from approximately 2.5 wt. % and 65 from 69 wt. %, respectively. Other elements vary unsystematically. In argillite, unaltered rocks contain 3 to 4 wt. % Na₂O, with similar amounts of K₂O, whereas albitized argillite has Na₂O up to 9.4 wt. %, with almost no K₂O (Table 5).

For both argillites and dykes, unaltered samples considered to closely represent pre-alteration bulk compositions were also analysed to allow calculations of gains and losses accompanying metasomatism. This was done using the method of Gresens (1967), which explicitly considers changes in volume attendant on alteration. Volume changes on alteration are denoted by the departure of a calculated 'volume factor' (F_V) from unity, with $F_V < 1$ indicating volume loss, and $F_V > 1$, volume increase. TiO₂ and Al₂O₃ were chosen as the immobile 'reference' components, and both yielded volume factors very near to one. As primary igneous textures are well-preserved in altered dykes, and sedimentary banding in argillite, this result gave additional confidence in the calculated mass changes. The results of mass balance calculations (Table 6) yield results consistent with the changes in composition discussed above, with losses of SiO₂ and K₂O, and large gains in Na₂O in aegirine- and riebeckite-bearing samples. The

albite-rich sample 5-10-3A, which lacks sodic amphibole or pyroxene, differs in having apparently experienced a slight addition of SiO₂. Other components are not consistently enriched or depleted, although Fe was added in most cases. Calculated mass balances in argillite are generally similar, although loss of SiO₂ appears to be minor (Table 6).

Trace elements typical of Mother Lode-type gold deposits (e.g. Kerrich, 1983), including Au, Ag, As, and Sb, are weakly to moderately enriched in albite-pyrite altered rocks (Table 7). Aegirine- and riebeckite-bearing samples are, for the most part, only slightly enriched in these components (Table 7).

Discussion

Composition of the metasomatic fluid. The metasomatic mineral assemblages, combined with the compositional changes accompanying alteration, allow constraints to be placed on the chemistry of the metasomatic fluids. As the actual compositions of the Na-pyroxenes and amphiboles are mostly far removed from those of idealized end-members, exact calculations of the activity of different species are not possible. The relationships of the metasomatic phases to variation in fluid a_{Na^+}/a_{H^+} , a_{Na^+}/a_{K^+} , and $a_{H_4SiO_4}$ are therefore shown schematically in Fig. 7. As both magnetite and hematite are present, all calculations were performed with f_{O_2} fixed by the magnetite-hematite buffer. Note that all diagrams are for end-

TABLE 4. Compositions of fresh and Na-metasomatized dykes in the Moccasin area

Sample	Fresh ¹	5-10-3A	5-10-2C	5-10-2D
SiO ₂	69.0	69.7	65.8	64.7
TiO ₂	0.40	0.39	0.44	0.40
Al ₂ O ₃	16.50	16.30	17.20	16.40
Fe ₂ O ₃	1.51	1.42	2.31	3.35
MgO	0.70	0.43	1.03	1.09
CaO	3.45	0.12	1.21	1.78
Na ₂ O	5.0	9.9	11.4	11.3
K ₂ O	2.43	0.09	0.12	0.19
P ₂ O ₅	0.15	0.14	0.15	0.15
LOI	0.39	1.47	0.39	0.62
Rb	60	20	20	10
Sr	190	80	200	190
Ba	360	460	360	440
Nb	20	30	20	10
Zr	130	230	130	180

(1) average analysis of three unaltered plagioclase-hornblende porphyritic dykes in Melones and Bear Mountain fault zones

(2) all analyses by X-ray fluorescence, X-ray Assay Laboratories, Don Mills, Ontario

(3) 5-10-3A = albitite (quartz-bearing) with minor pyrite, chlorite; 5-10-2C = riebeckite-aegirine albitite; 5-10-2D = aegirine albitite

member compositions, and were computed using thermochemical data from a variety of sources (see figure caption). As can be seen in Fig. 7, the sequence albitite-chlorite (pyrite-Fe oxide) → albitite-riebeckite → albitite-aegirine corresponds to increasing $a_{\text{Na}^+}/a_{\text{H}^+}$. The local occurrence of analcime-paragonite indicates that the metasomatic fluid was

quartz-undersaturated at times (Fig. 7). The assemblages albitite-riebeckite and albitite-aegirine are not incompatible with quartz-saturated fluids, but as noted above, quartz is absent in Na-amphibole and -pyroxene-bearing rocks, suggesting that quartz-undersaturation was common. This is in accord with evidence of silica loss during metasomatism, as

TABLE 5. Composition of fresh and albitized argillite, Jamestown area¹

Sample	R3379 ²	R3382 ²	RL-12-76 ³	R3376 ³	R3380 ³
SiO ₂	52.3	50.7	57.7	64.7	56.3
TiO ₂	0.81	—	0.81	—	—
Al ₂ O ₃	15.9	16.1	15.7	13.8	13.0
Fe ₂ O ₃	0.86	1.8	6.4	4.7	6.3
FeO	3.4	2.8	—	0.6	0.3
MgO	2.2	2.6	3.0	2.0	3.3
CaO	4.4	5.0	0.07	0.03	1.6
Na ₂ O	4.0	3.2	9.4	9.0	8.1
K ₂ O	3.4	3.7	0.1	0.06	0.05
P ₂ O ₅	—	—	0.03	—	—
LOI	—	—	3.5	—	—
Total	87.27	85.9	96.68	94.89	88.95

(1) Analyses from Lamarre (1977) by Skyline Laboratories, Wheatridge Colorado

(2) relatively fresh argillite, some dolomite alteration

(3) albitized argillite

TABLE 6. Calculated gains and losses in Na-altered dykes, Moccasin area

Sample S.G.	Ref 2.65	5-10-2C 2.65	5-10-2D 2.65	5-10-3A 2.65
g/100cc ¹				
SiO ₂	182.85	174.37	171.46	184.71
TiO ₂	1.06	1.17	1.06	1.03
Al ₂ O ₃	43.73	45.58	43.46	43.20
Fe ₂ O ₃	3.98	6.12	8.88	3.76
MgO	1.86	2.73	2.89	1.14
CaO	9.28	3.21	4.72	0.32
Na ₂ O	13.25	30.21	29.95	26.24
K ₂ O	6.63	0.32	0.50	0.24
P ₂ O ₅	0.40	0.40	0.37	0.37
LOI	1.03	1.03	1.64	3.90
mg/100cc ¹				
Rb	15.90	5.30	2.65	5.30
Sr	50.35	50.35	53.00	21.20
Ba	95.40	95.40	116.60	121.90
Nb	5.30	5.30	2.65	7.95
Zr	34.45	34.45	47.70	60.95
Fv _{Al} ²				
	1.0	0.96	1.01	1.01
Fv _{Ti} ²				
	1.0	0.91	1.0	1.03
Fv _{Ave} ²				
	1.0	0.93	1.00	1.02
change ³				
SiO ₂	0.0	-19.95	-10.87	5.36
TiO ₂	0.0	0.03	0.00	-0.01
Al ₂ O ₃	0.0	-1.14	-0.13	0.29
Fe ₂ O ₃	0.0	1.74	4.93	-0.14
MgO	0.0	0.69	1.04	-0.69
CaO	0.0	-6.28	-4.54	-8.95
Na ₂ O	0.0	14.97	16.78	13.48
K ₂ O	0.0	-6.33	-6.12	-6.38
P ₂ O ₅	0.0	-0.03	-0.03	-0.02

(1) abundances of components in samples expressed as weight per unit volume

(2) Fv = volume factor as defined in Gresens (1967) for subscripted component

(3) gains or loss of component expressed as grams per 100 cm³ of original rock

illustrated by the mass balance calculations (Table 6).

Origin of Na-metasomatized zones. Albite-aegirine-riebeckite assemblages, as documented at Moccasin, are most common in felsic peralkaline rocks (e.g. Williams *et al.*, 1982) and in fenitized zones which commonly surround alkalic intrusions (Platt and Woolley, 1990; Morgan and Woolley, 1988). They are also locally present in metamorphosed oxidized, iron-rich rocks (e.g. Miyano and Klein,

TABLE 7. Abundance of gold and other trace metals in Na-altered samples, Jamestown and Moccasin areas

Sample	Lithology	Au	Ag	As	Sb
AC-428	1	0.028	<5	76	2.4
AC-434	1	0.003	<5	19	1.1
5-10-2C	2	<0.010	<0.5	<2	0.5
5-10-2D	3	0.020	<0.5	<2	<0.4
5-10-3A	4	0.078	20.0	99	0.5
5-10-4A	5	0.014	<5	120	2.1

Analyses by INAA, Neutron Activation Services, Hamilton, Ontario, all analyses in ppm

Lithology, 1 = albite-pyrite altered argillite, 2 = albite-riebeckite-aegirine altered dyke, 3 = albite-aegirine altered dyke, 4 = albite-pyrite-chlorite altered dyke, 5 = riebeckite-albite altered argillite.

1983). Metasomatic formation of aegirine- and/or riebeckite-bearing albitite not related to alkalic magmatism has also been documented in a few localities, commonly associated with uranium mineralization. In these cases, as in the Moccasin area, the Na-metasomatized rocks are associated with major faults, either steeply-dipping (Omelyanenko and Mineyeva, 1982), or thrust faults (Lobato *et al.*, 1983 *a,b*). An association with shear zone-hosted gold deposits has been noted elsewhere (Morasse *et al.*, 1988), but appears to be uncommon. Somewhat enigmatic occurrences of riebeckite- and aegirine-bearing metamorphic rocks are documented in Aberdeenshire (McLachlan, 1951), hosted by Moine or Lewisian metamorphic rocks. The host rocks are of much higher metamorphic grade than those discussed here (kyanite grade), and the sodic minerals apparently occur in close association with 'soda-pegmatite' (McLachlan, 1951).

Garson *et al.* (1984) describe Na-metasomatized rocks from a number of locations along the Great Glen Fault, where Moine metamorphic rocks, Caledonian granites, and carbonate rocks have been affected by albitization and formation of sodic amphibole (crocidolite) and aegirine. They attribute the metasomatic alteration to fenitization by carbonatites emplaced along the Great Glen Fault. Garson *et al.* (1984) provide analytical data for several examples of carbonate-rich veins they classify as carbonatite. Most of these have a number of characteristics that suggest a non-carbonatite origin, including ⁸⁷Sr/⁸⁶Sr ratios ranging from 0.7095 to 0.7201, and REE concentrations and ratios that differ from most carbonatites. Garson *et al.*

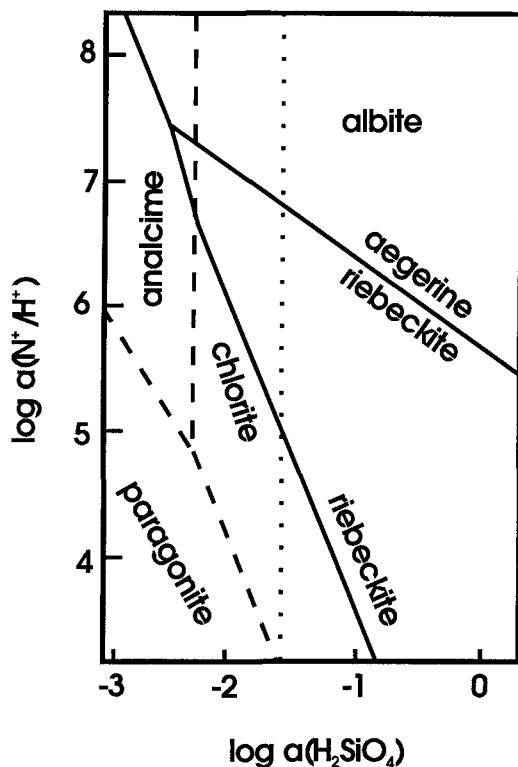


FIG. 7. Stability relationships of selected minerals in the system $\text{Na}_2\text{O}-\text{Al}_2\text{O}_3-\text{Fe}_2\text{O}_3-\text{SiO}_2-\text{H}_2\text{O}$ in terms of $\log a_{\text{H}_2\text{SiO}_4}$ vs $\log (a_{\text{Na}^+}/a_{\text{H}^+})$, at 300° and 2 kb with f_{O_2} fixed by the magnetite-hematite buffer. Dashed lines indicate equilibria in the sub-system $\text{Na}_2\text{O}-\text{Al}_2\text{O}_3-\text{SiO}_2-\text{H}_2\text{O}$. Quartz saturation indicated by dotted vertical line. The sequence chlorite (chl) \rightarrow riebeckite (rieb) \rightarrow aegirine (aeg) corresponds to increasing $a_{\text{Na}^+}/a_{\text{H}^+}$. As shown, aegirine and riebeckite are not incompatible with quartz stability, but the local occurrence of analcime and paragonite, combined with the absence of quartz in aegirine- and riebeckite-bearing zones suggests undersaturation in SiO_2 . Note that the diagram is calculated for pure mineral compositions, and that equilibria for actual mineral compositions will be somewhat displaced. Thermochemical data from Helgeson (1969), Helgeson and Kirkham (1976), Helgeson *et al.* (1979), and Miyano and Klein (1983).

(1984) also suggest that the occurrence of albitites in their study area, particularly a uranium-rich occurrence, requires a carbonatite source. Metasomatic albitites, sufficiently uranium-rich to constitute ore and with no relationship to alkalic magmatism, are, however, well-documented in Brazil (Lobato *et al.*, 1983 *a,b*), and the former USSR (Omel'yanenko and Mineyeva, 1982).

In the case of the altered dykes in the Moccasin area, chondrite-normalized *REE* patterns of both altered and fresh rocks (Fig. 8) are characterized by moderate negative slopes and small negative or positive Eu anomalies. This, along with the overall composition of the dykes (Table 5), suggests that the igneous rocks along the Melones Fault are of calc-alkalic affinity, and that the Na-amphibole and pyroxene are not of primary igneous origin, or the products of fenitization.

Role of ultramafic rocks in Na-metasomatism. The association between altered ultramafic rocks and sodium-metasomatized zones has been noted in a number of other areas (e.g. Böhlke, 1986, 1989; Coveney, 1981; Francis, 1955). A common feature of altered ultramafic rocks along major faults is the development of quartz-magnetite assemblages, in which Cr-muscovite (locally referred to as fuchsite or mariposite) is a typical accessory phase. Such Cr-muscovites contain as much as 7 to 8 wt. % Cr_2O_3 , and are also commonly K-deficient (Table 8). Assuming ideal mixing, a_{musc} in such micas is in the range 0.24–0.30. Obviously, the equilibrium between white mica and albite, which seems to control hydrothermal fluid composition in many shear zone-related gold deposits, will be significantly displaced, such that Cr-rich white mica could form in ultramafic rocks from fluids which are within the albite-stable field (for stoichiometric muscovite) in terms of $a_{\text{Na}^+}/a_{\text{K}^+}$ (Fig. 9). The result of this formation of muscovite outside of its end-member stability field will be an increase in fluid $a_{\text{Na}^+}/a_{\text{K}^+}$, such that when the fluid encounters a quartzofeldspathic rock (which lacks Cr to stabilize muscovite), albitization will result. In addition, higher fluid $a_{\text{Na}^+}/a_{\text{H}^+}$ may result from interaction with ultramafic rocks, as many alteration reactions in ultramafic rocks consume CO_2 . The formation of talc-rich zones along the margins of many serpentinite bodies is the result of SiO_2 addition to the ultramafic rocks (Chidester, 1962; Albino, 1990), and could result in fluids with $a_{\text{H}_2\text{SiO}_4}$ less than quartz saturation. The occurrence of marialitic scapolite, which implies salinities of at least 20% (Vanko and Bishop, 1982), is difficult to reconcile with the low salinities considered typical of fluids in these hydrothermal systems (e.g. Kerrich, 1983), but extensive involvement of originally low-salinity fluids in hydration reactions (perhaps as relict olivine in peridotite is consumed) may account for such compositions.

The ultimate source for the metasomatic fluids is not resolved by the present study, but stable isotopic compositions of both albitized and carbonate-altered zones elsewhere along the Melones Fault Zone and related structures (e.g. Böhlke and Kistler, 1986; Weir and Kerrick, 1987; Taylor, 1986) indicate fluids had $\delta^{18}\text{O}$ of 8 to 14‰, with δD -10 to -50 ‰. These

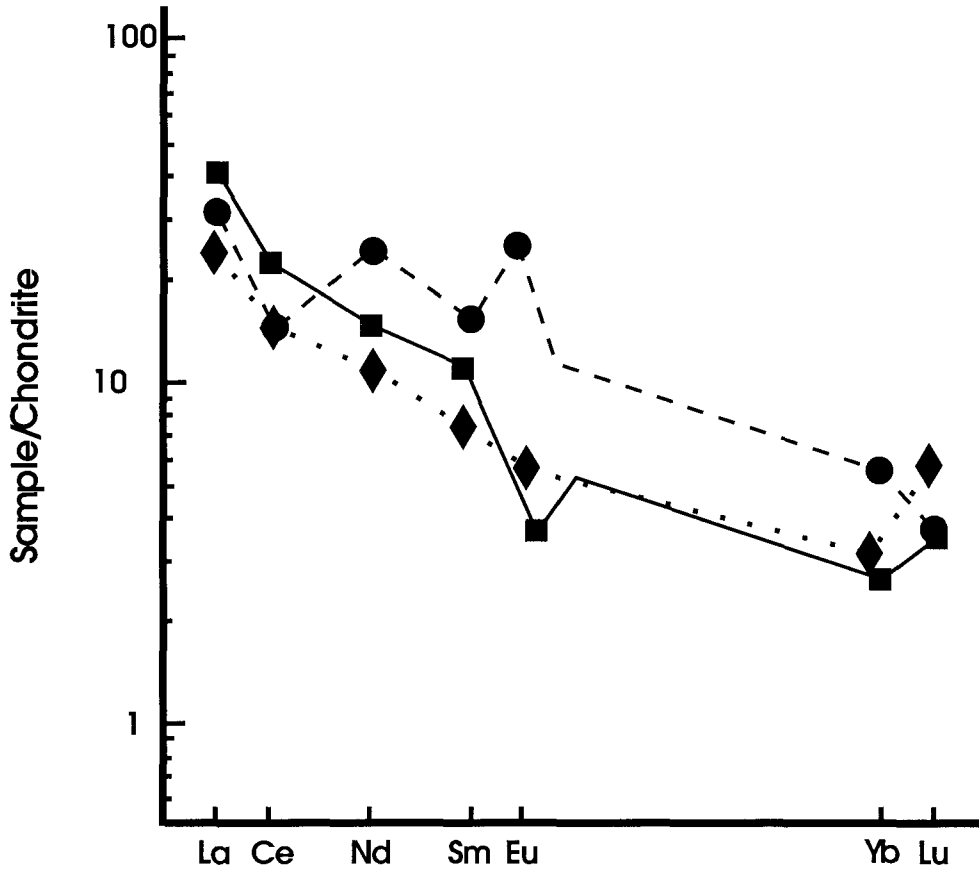


FIG. 8. Chondrite-normalized (after Masuda *et al.*, 1973) rare earth element patterns for unaltered (■) and altered (◆, ●) dykes from Moccasin area.

data are most consistent with a metamorphic origin for these fluids. The timing of metasomatism in other areas along the Melones Fault Zone (Böhlke and Kistler, 1986) is consistent with derivation of fluids by devolatilization related to batholith emplacement. The unusual fluid compositions documented here are probably the result of extensive reaction of the fluid with wallrocks, especially peridotites and their serpentinized equivalents, as the fluids ascended along the fault.

Conclusions

Metasomatic assemblages comprising albite (quartz-chlorite-pyrite), albite-riebeckite-aegirine, and albite-aegirine have been produced by Na_2O metasomatism, commonly with associated loss of

K_2O and SiO_2 , of originally quartzo-feldspathic and low-grade pelitic rocks. The fluid responsible was CO_2 -poor, alkaline, and had high Na^+/K^+ . The process was isovolumetric, resulting in textural preservation of the protoliths. Intermediate to felsic dykes, which are locally altered to the Na-rich assemblages, have normal calc-alkaline compositions, and no alkaline rocks are known in the area. The sodium-metasomatic event pre-dated, but has a close spatial association with, Au-bearing zones with white mica- and carbonate-bearing assemblages. The albite zones in this study, in common with many other Na-metasomatized zones along faults, are located adjacent to altered ultramafic rocks, and interaction of a fluid, originally in equilibrium with albite+muscovite, with ultramafic rocks may have been responsible for production of the albitizing fluid.

TABLE 8. Compositions of Cr-bearing muscovite from altered ultramafic rocks of the Mother Lode Belt

Sample	V-1	V-1	V-1	V-1	V-1	6-21-2K	AC-421	AC-424						
SiO ₂	48.05	48.71	59.23	47.77	47.82	48.09	48.99	46.62	47.90	47.85	48.95	48.85	48.85	48.95
TiO ₂	0.02	0.02	0.01	0.03	0.00	0.02	0.01	0.01	0.00	0.01	0.07	0.06	0.06	0.07
Al ₂ O ₃	28.33	26.37	20.87	27.03	27.43	26.80	27.57	28.69	28.73	26.48	27.04	25.10	25.10	27.04
Cr ₂ O ₃	5.18	7.64	4.98	6.98	6.06	5.38	5.00	3.30	4.25	7.77	4.74	7.58	7.58	4.74
MnO	0.08	0.11	0.06	0.07	0.00	0.05	0.03	0.00	0.06	0.04	0.07	0.36	0.36	0.07
FeO	0.22	0.19	0.24	0.26	0.38	0.49	0.48	0.33	0.39	0.46	0.23	0.36	0.36	0.23
MgO	1.89	2.21	1.84	2.04	2.50	2.24	2.34	2.24	2.09	2.14	2.23	2.26	2.26	2.23
Na ₂ O	0.05	0.05	0.07	0.04	0.10	0.05	0.11	0.13	0.10	0.08	0.18	0.13	0.13	0.18
K ₂ O	7.38	6.82	5.50	6.83	7.18	7.36	7.54	7.17	7.65	7.69	8.45	7.82	7.82	8.45
CaO	0.11	0.08	0.11	0.05	0.12	0.03	0.05	0.03	0.01	0.00	0.00	0.00	0.00	0.00
BaO	0.03	0.04	0.03	0.00	0.04	0.06	0.07	0.03	0.03	0.02	-	-	-	-
Total	91.32	92.23	92.95	91.10	91.59	90.55	92.19	88.59	91.21	92.55	91.96	92.23	92.23	91.96
cations on the basis of 22 O														
Si	6.592	6.647	7.754	6.589	6.564	6.667	6.665	6.560	6.577	6.560	6.706	6.717	6.717	6.706
Ti	0.002	0.002	0.001	0.003	0.000	0.002	0.001	0.001	0.000	0.001	0.007	0.006	0.006	0.007
Al	4.582	4.242	3.221	4.396	4.439	4.380	4.422	4.759	4.651	4.280	4.367	4.069	4.069	4.367
Cr	0.562	0.824	0.515	0.761	0.658	0.590	0.538	0.367	0.461	0.842	0.513	0.824	0.824	0.513
Mn	0.009	0.013	0.007	0.008	0.000	0.006	0.003	0.000	0.007	0.005	0.008	0.008	0.008	0.008
Fe	0.032	0.028	0.034	0.038	0.056	0.073	0.070	0.050	0.057	0.068	0.026	0.041	0.041	0.026
Mg	0.386	0.449	0.359	0.419	0.511	0.463	0.474	0.470	0.428	0.437	0.455	0.463	0.463	0.455
Na	0.013	0.013	0.018	0.011	0.027	0.013	0.029	0.035	0.027	0.021	0.048	0.035	0.035	0.048
K	1.292	1.187	0.919	1.202	1.257	1.302	1.309	1.287	1.340	1.345	1.477	1.372	1.372	1.477
Ca	0.016	0.012	0.015	0.007	0.018	0.004	0.007	0.005	0.001	0.000	0.000	0.000	0.000	0.000
Ba	0.001	0.002	0.002	0.000	0.000	0.002	0.004	0.004	0.002	0.002	-	-	-	-

Analyses by electron microprobe, University of Western Ontario

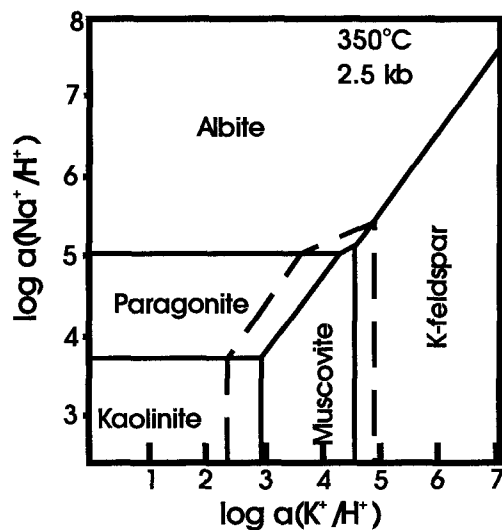


FIG. 9. Calculated stability relations for selected minerals in the system $\text{Na}_2\text{O}-\text{K}_2\text{O}-\text{Al}_2\text{O}_3-\text{SiO}_2-\text{H}_2\text{O}$ in terms of $\log(a_{\text{Na}^+}/a_{\text{H}^+})$ vs $\log(a_{\text{K}^+}/a_{\text{H}^+})$ at 350°C and 2.5 kbar. Stability field for muscovite shown for end-member composition (solid lines) and with $a_{\text{musc.}} = 0.30$ (dashed lines). Note expansion of muscovite field into albite-stable field for mineral compositions removed from end-member. Diagram calculated using thermochemical data and computer programs of Berman 1988, and Berman *et al.* 1987.

Acknowledgements

Financial support for this study was provided by BP Minerals of Canada. Assistance with microprobe analysis by R.L. Barnett is appreciated. Comments by two journal reviewers helped clarify the presentation.

References

- Albino, G.V. (1990) *Structural setting, geochemistry, and large-scale metal zoning in Mother Lode-type deposits*. Unpub. Ph.D. thesis, Univ. Western Ontario, London, Canada.
- Albino, G.V. (1993) In *Basement Tectonics*, 7 (Mason, R., ed.), Kluwer, Amsterdam, 289–303.
- Berman, R.G. (1988) Internally consistent thermodynamic data for minerals in the system $\text{Na}_2\text{O}-\text{K}_2\text{O}-\text{CaO}-\text{MgO}-\text{FeO}-\text{Fe}_2\text{O}_3-\text{Al}_2\text{O}_3-\text{SiO}_2-\text{TiO}_2-\text{H}_2\text{O}-\text{CO}_2$. *J. Petrol.*, **29**, 445–522.
- Berman, R.G., Brown, T.H. and Perkins, E.H. (1987) GEO-CALC: Software for calculation and display of P-T-X phase diagrams. *Amer. Mineral.*, **72**, 861–2.
- Böhlke, J.K. (1986) *Local wall rock control of alteration and mineralization reactions along discordant gold quartz veins, Alleghany, California*. Unpub. Ph.D. thesis, University of California, Berkeley, Berkeley, California.
- Böhlke, J.K. (1989) *Econ. Geol.*, **84**, 291–327.
- Böhlke, J.K. and Kistler, R.W. (1986) *Econ. Geol.* **81**, 296–322.
- Card, K.D., Poulsen, K.H., and Robert, F. (1989) In *The geology of gold deposits; the perspective in 1988* (Keays, R.R., Ramsay, W.R.H., and Groves, D.I., eds.) *Economic Geology Monograph* **6**, 19–36.
- Chidester, A.H. (1962) Petrology and geochemistry of selected talc-bearing ultramafic rocks and adjacent country rocks in north-central Vermont. *U.S. Geol. Surv. Prof. Pap.* **345**, 207 pp.
- Clark, L.D. (1960) *Geol. Soc. Am. Bull.* **71**, 483–96.
- Colvine, A.C. (1989) In *The geology of gold deposits; the perspective in 1988* (Keays, R.R., Ramsay, W.R.H., and Groves, D.I., eds.) *Economic Geology Monograph* **6**, 37–53.
- Couture, J-F. and Pilote, P. (1993) *Econ. Geol.* **88**, 1664–84.
- Coveney, R.M. Jr. (1981) *Econ. Geol.* **76**, 2176–99.
- Francis, G. (1955) *Geol. Mag.* **92**, 433–47.
- Garson, M.S., Coats, J.S., Rock, N.M.S., and Deans, T. (1984) *Q. Jour. Geol. Soc. London*, **141**, 711–32.
- Gresens, R.L. (1967) *Chem. Geol.*, **2**, 47–65.
- Groves, D.I., Barley, M.E., and Ho, S.E. (1989) In *The geology of gold deposits; the perspective in 1988* (Keays, R.R., Ramsay, W.R.H., and Groves, D.I., eds.) *Economic Geology Monograph* **6**, 71–85.
- Helgeson, H.C. (1969) *Amer. J. Sci.*, **267**, 729–804.
- Helgeson, H.C. and Kirkham, D.H. (1976) *Amer. J. Sci.*, **276**, 97–240.
- Helgeson, H.C., Delany, J.M., Nesbitt, H.W. and Bird, D.K. (1979) *Amer. J. Sci.*, **278-A**, 1–229.
- Kerrich, R. (1983) Geochemistry of gold deposits in the Abitibi greenstone belt. *Can. Inst. Mining and Metal. Special Paper* **27**, 75 pp.
- Kishida, A. and Kerrich, R. (1987) *Econ. Geol.*, **82**, 649–90.
- Knopf, A. (1929) The Mother Lode system of California. *U.S. Geol. Surv. Prof. Pap.*, **157**.
- Lamarre, R.A. (1977) *Geology of the Alabama-Crystal-line Mines, Mother Lode gold belt, California*. Unpub. M.Sc. thesis, University of Western Ontario, London.
- Leake, B.E. (1978) *Canad. Mineral.*, **16**, 501–20.
- Leonardos, O.H., Jr. and Fyfe, W.S. (1967) *Amer. J. Sci.*, **265**, 609–18.
- Lobato, L.M., Forman, J.M.A., Fuzikawa, K., Fyfe, W.S. and Kerrich, R. (1983a) *Canad. Mineral.*, **21**, 647–54.
- Lobato, L.M., Forman, J.M.A., Fyfe, W.S., Kerrich, R. and Barnett, R.L. (1983b) *Nature*, **303**, 235–7.
- McLachlan, G.R. (1951) *Mineral. Mag.*, **29**, 476–95.
- Masuda, A., Nakamura, N. and Tanaka, T. (1973) *Geochim. Cosmochim. Acta*, **37**, 239–48.

- Miyano, T. and Klein, K. (1983) *Amer. Mineral.*, **68**, 517–29.
- Morasse, S., Hodgson, C.J., Guha, J. and Coulombe, A. (1988) In *Bicentennial gold 88; extended abstracts, poster programme* (Goode, A.D.T., Smyth, E.L., Birch, W.D. and Bosma, L.I., eds.) *Abstracts, Geol. Soc. Austral.*, **23**, 92–4.
- Morogan, V. and Woolley, A.R. (1988) *Contrib. Mineral. Petrol.*, **100**, 169–82.
- Okay, A.I. (1980) *J. Geol.*, **88**, 225–32.
- Omel'yanenko, B.I. and Mineyeva, I.G. (1982) *Inter. Geol. Rev.*, **24**, 422–30.
- Papike, J.J. and White, C. (1979) *Geophys. Res. Letters*, **6**, 913–16.
- Platt, R.G. and Woolley, A.R. (1990) *Canad. Mineral.*, **28**, 241–50.
- Ransome, F.L. (1900) Description of the Mother Lode district [California]. *U.S. Geol. Surv. Geol. Atlas, Folio*, **63**.
- Robinson, P., Spear, F.S., Schumacher, J.C., Laird, J., Klein, C., Evans, B.W. and Doolan, B.L. (1982) In *Amphiboles: petrology and experimental phase relations* (Veblen, D.R. and Ribbe, P.H., eds.) *Rev. Mineral.*, **9B**, 1–227.
- Saleeby, J.B., Geary, E.E., Paterson, S.R. and Tobisch, O.T. (1989) *Geol. Soc. Amer. Bull.*, **101**, 1481–92.
- Taylor, B.E. (1986) In *Gold '86, An International Symposium on the Geology of Gold Deposits*, Poster Volume (Chater, A.M., ed.), 148–50.
- Turner, H.W. (1896) *Amer. Geol.*, **17**, 375–86.
- Vanko, D.A. and Bishop, F.C. (1982) *Contrib. Min. Pet.*, **81**, 277–89.
- Weir, R.H. Jr. and Kerrick, D.M. (1987) *Econ. Geol.*, **82**, 328–44.
- White, A.J.R. (1962) *J. Petrol.*, **3**, 38–48.
- Williams, H., Turner, F.J. and Gilbert, C.M. (1982) *Petrography; an introduction to the study of rocks in thin sections*. W.H. Freeman and Company, San Francisco, 626 pp.

[Manuscript received 8 April 1994:
revised 16 September 1994]